An Improved Mumford-Shah Model and Its Applications to Image Processing with the Piecewise Constant Level Set Method

SONG Jin-Ping[1] LI Shuai-Jie[1]

Abstract For quick segmentation and denoising, the classical Mumford-Shah (MS) model needs to enhance the penalization term, *i.e.* to increase the penalization parameter, which leads to gradual disappearance of objects. In this paper, we propose an improved Mumford-Shah (IMS) model to avoid the phenomenon, and adopt the piecewise constant level set method (PCLSM) and the gradient descent method to solve the minimization problem. Numerical experiments are given to show the efficiency and advantages of the new model and the algorithms.

Key words Segmentation, denoising, Mumford-Shah model, level set, piecewise constant level set method (PCLSM)

1 Introduction

Level set methods, originally introduced by Osher and Sethian[1], have been developed into one of the most successful tools for the computation of evolving geometries and have found many practical applications. They use the zero level sets of some functions to trace interfaces that separate a domain Ω into subdomains. For a recent survey on the level set methods, see [2∼4].

In [5∼7] some variants of the level set methods of [1], the so-called piecewise constant level set method (PCLSM)[5], are proposed. The methods can be used for different purposes. In [8, 9], their applications to inverse problems involving elliptic and reservoir equations are shown. In [5∼7, 10], the ideas are also used for image segmentation.

Image segmentation and denoising are the foundational tasks of computer vision. Its goal is to partition a given image into regions that contain distinct objects. One of the most common forms of segmentation is based on the assumption that distinct objects in an image have different approximately constant (or slowly varying) colors. When using the Mumford-Shah (MS) model[11] for image segmentation and denoising with PCLSM, the iterative number has to be very large, and the convergence speed is also very slow. In order to achieve the aim of quick segmentation and denoising, we have to enhance the penalization term, *i.e.*, to enlarge the parameter β. Hence, the boundary of object gets smoother, and the interface gets shorter. If we continue to increase β, the object will disappear. In this work, we will improve the penalization term of the Mumford-Shah model to overcome this shortcoming. Experiments show that the improved Mumford-Shah (IMS) model makes the algorithms more stable and the result of segmentation better at a fast convergence rate than that of the MS model.

2 Mumford-Shah model with PCLSM

First, we shall recall PCLSM of [5]. The essential idea of PCLSM of [5] is to use a piecewise constant level set function to identify the subdomains. Partition the domain Ω into subdomains Ω_i, where $i = 1, 2, \cdots, n$, and assume that the number n of the subdomains is known. In order to identify the subdomains, we identify a piecewise constant level set function φ

$$\varphi(x) = i, \quad x \in \Omega_i, \quad i = 1, 2, \cdots, n \tag{1}$$

Then, for any given partition $\{\Omega_i\}_i^n$ of the domain Ω, it corresponds to a unique piecewise constant level set function φ which takes values $1, 2, \cdots, n$, associated with such a level set function φ. The characteristic functions $\psi_i(x)$ of the subdomains are given below

$$\psi_i(x) = \frac{1}{\alpha_i} \prod_{j=1, j\neq i}^{n} (\varphi(x) - j), \quad \alpha_i = \prod_{k=1, k\neq i}^{n} (i - k) \tag{2}$$

If function φ is given in (1), then we have $\psi_i(x) = 1$ for $x \in \Omega_i$, and $\psi_i(x) = 0$ elsewhere. We can use the characteristic functions to extract geometrical information for the subdomains and the interfaces between the subdomains. For example,

$$\text{Length}\,(\partial\Omega_i) = \int_{\Omega_i} |\nabla\psi_i(x)|\mathrm{d}x, \quad \text{Area}\,(\Omega_i) = \int_{\Omega_i} \psi_i(x)\mathrm{d}x \tag{3}$$

A constraint is introduced to make φ a piecewise constant function and to ensure uniqueness at convergence

$$K(\varphi) = (\varphi - 1)(\varphi - 2)\cdots(\varphi - n) = \prod_{i=1}^{n}(\varphi - i) \tag{4}$$

At every point in Ω, the level set function φ satisfies

$$K(\varphi) = 0 \tag{5}$$

There exists a unique $i \in \{1, 2, \cdots, n\}$ for every $x \in \Omega$ such as $\varphi(x) = i$. This means that any point x belongs to one and only one phase or region. Thus, the constraint is introduced to guarantee that there is no vacuum and no overlap between regions.

The level set idea has been used for Mumford-Shah image segmentation in [5]. For a given digital image, $u_0 : \Omega \mapsto \mathbf{R}$ that may be corrupted by noise and blurred. Note that a function u given by

$$u = \sum_{i=1}^{n} c_i\psi_i \tag{6}$$

is a piecewise constant function and $u = c_i$ in Ω_i, if φ is as given in (1). In this way, the function u is a sum of unknown constants c_i multiplied by polynomials ψ_i.

Received January 23, 2007; in revised form May 11, 2007
Supported by National Natural Science Committee and Chinese Engineering Physics Institute Foundation (10576013), Natural Science Foundation of Henan Province (0611053200), Natural Science Study Foundation of Henan University (06YBZR028)
1. Institute of Applied Mathematics, College of Mathematics and Information Science, Henan University, Kaifeng 475004, P. R. China
DOI: 10.1360/aas-007-1259

Based on the definitions and observations above, the following constrained minimization problem has been introduced to segment and denoise an image u_0 in [5]

$$\min_{c,\varphi,K(\varphi)=0}\{F(c,\varphi)=\frac{1}{2}\int_{\Omega}|u-u_0|^2\mathrm{d}x+\beta\sum_{i=1}^{n}\int_{\Omega_i}|\nabla\psi_i|\mathrm{d}x\} \tag{7}$$

The term $\frac{1}{2}\int_{\Omega}|u-u_0|^2\mathrm{d}x$ will penalize large approximation errors. We see that the other term, the penalization, is the sum of the lengths of the boundaries of the subdomains, and the parameter β is introduced to control the effect of the term, and β is found by trial and error. Choosing a large β will shorten the lengths of the boundaries and increase the smooth speed. But decreasing β will give birth to longer boundaries and slower speed.

3 Improvement of the Mumford-Shah model

Experiments revealed that, to attain fast convergence and a good smooth result and segmentation of a noised image by the classic Mumford-Shah model, we have to enhance the penalization term, but so doing will lead to the degeneration of images, and make the equation lose stabilization.

To accomplish segmentation and denoising, we only need to smoothen the interior of the objects, and preserve their shapes and edges. It is essential to improve the penalization term structure. In order to get a good understanding of the influence of the penalization term, let us consider the following constrained minimization problem[12]

$$\min_{c,\varphi,K(\varphi)=0}\{F(c,\varphi)=\frac{1}{2}\int_{\Omega}|u-u_0|^2\mathrm{d}x+\beta\sum_{i=1}^{n}\int_{\Omega_i}\omega(|\nabla\psi_i|)\mathrm{d}x\} \tag{8}$$

We need to find the properties of ω so that the solution of the minimization problem is close to a piecewise constant image, formed by homogeneous regions separated by sharp edge.

Suppose that $F(c,\varphi)$ has a minimum point u. Then it formally satisfies the Euler-Lagrange equation

$$(u-u_0)\frac{\partial u}{\partial\varphi}-\beta\sum_{i=1}^{n}\nabla\cdot(\frac{\omega'(\nabla\psi_i)}{|\nabla\psi_i|}\nabla\psi_i)\frac{\partial\psi_i}{\partial\varphi}=0 \tag{9}$$

(9) can be written in an expanded form by formally developing the divergence term.

We are going to show that it can be decomposed using the local image structures, that is, the tangent and normal directions to the isophote lines (Lines along which the intensity is constant). More precisely, for each point x where $|\nabla\psi_i(x)|\neq 0$, we can define the vectors $\boldsymbol{N}(x)=\frac{\nabla\psi_i(x)}{|\nabla\psi_i(x)|}$ and $\boldsymbol{T}(x)$, $|\boldsymbol{T}(x)|=1$, with $\boldsymbol{T}(x)$ orthogonal to $\boldsymbol{N}(x)$. With the usual notation, $\psi_{ix_1},\psi_{ix_2},\psi_{ix_1x_1}\cdots$, for the first and second partial derivatives of $\psi_i(x)$, we can rewrite (9) as

$$(u-u_0)\frac{\partial u}{\partial\varphi}-\beta\sum_{i=1}^{n}(\frac{\omega'(|\nabla\psi_i|)}{|\nabla\psi_i|}\psi_{iTT}+\omega''(|\nabla\psi_i|)\psi_{iNN})\frac{\partial\psi_i}{\partial\varphi}=0 \tag{10}$$

where ψ_{iTT} and ψ_{iNN} denote the second derivatives of ψ_i in the $\boldsymbol{T}$ direction and $\boldsymbol{N}$ direction, respectively

$$\psi_{iTT}={}^t\boldsymbol{T}\nabla^2\psi_i\boldsymbol{T}=\frac{1}{|\nabla\psi_i|^2}(\psi_{ix1}^2\psi_{ix2x2}+\psi_{ix2}^2\psi_{ix1x1}-2\psi_{ix1}\psi_{ix1x2}) \tag{11}$$

$$\psi_{iNN}={}^t\boldsymbol{N}\nabla^2\psi_i\boldsymbol{N}=\frac{1}{|\nabla\psi_i|^2}(\psi_{ix1}^2\psi_{ix1x1}+\psi_{ix2}^2\psi_{ix2x2}-2\psi_{ix1}\psi_{ix1x2}) \tag{12}$$

In fact, decomposing the divergence term as a weighted sum of the two directional derivatives along $\boldsymbol{T}$ and $\boldsymbol{N}$ can be done for most classical diffusion operators[13]. This enables us to see clearly the action of the operators in the directions $\boldsymbol{T}$ and $\boldsymbol{N}$.

The function ω should satisfy the following conditions:

1) At location where the variations of the intensity are weak (low gradients), we should make the image smooth uniformly in all directions, assuming that the function ω is regular, this isotropic smoothing condition can be achieved by imposing

$$\omega'(0)=0,\quad \lim_{s\to0^+}\frac{\omega'(s)}{s}=\lim_{s\to0^+}\omega''(s)=\omega''(0)>0 \tag{13}$$

2) In the neighborhood of edges, the image presents a strong gradient. To preserve this edges, it is preferable to diffuse along the edges (in the $\boldsymbol{T}$ direction) and not across it. To do this, it suffices to annihilate the coefficient of ψ_{iNN} for strong gradients in (9) and to assume that the coefficient of ψ_{iTT} does not vanish

$$\lim_{s\to+\infty}\omega''(s)=0,\quad \lim_{s\to+\infty}\frac{\omega'(s)}{s}=\beta>0 \tag{14}$$

But these two conditions are incompatible. In order to preserve this edges, we let the $\omega''(s)$ and $\omega'(s)/s$ both converge to zero as $s\to+\infty$, but at different rates

$$\lim_{s\to+\infty}\omega''(s)=\lim_{s\to+\infty}\frac{\omega'(s)}{s}=0,\quad \lim_{s\to+\infty}\frac{\omega''(s)}{\omega'(s)/s}=0 \tag{15}$$

To sum up, we use new energy function (8), where the function must satisfy conditions (13) and (15).

4 Algorithms

In the following, we will use augmented Lagrangian method to solve constrained minimization problem (8), and use the classical gradient descent method to solve the minimization problem.

The augmented function for this minimization problem is defined as

$$L(c,\varphi,\lambda)=F(c,\varphi)+\int_{\Omega}\lambda K(\varphi)\mathrm{d}x+\frac{r}{2}\int_{\Omega}|K(\varphi)|^2\mathrm{d}x \tag{16}$$

where $\lambda\in L^2(\Omega)$ is the multiplier, and $r>0$ is a penalty parameter. We use the classical gradient descent method to solve the minimization problem.

Algorithm: (Gradient descent method) Choose initial values for φ^0 and λ^0. For $k=1,2,\cdots$, do:

1) Find c^k from

$$L(c^k,\varphi^{k-1},\lambda^{k-1})=\min_{c}L(c,\varphi^{k-1},\lambda^{k-1}); \tag{17}$$

2) Use (6) and update $u = \sum_{i=1}^{n} c_i^k \psi_i(\varphi^{k-1})$;

3) Find φ^k from

$$L(c^k, \varphi^k, \lambda^{k-1}) = \min_{\varphi} L(c^k, \varphi, \lambda^{k-1}) \tag{18}$$

4) Update $u = \sum_{i=1}^{n} c_i^k \psi_i(\varphi^k)$;

5) Update the Lagrangian-multiplier by

$$\lambda^k = \lambda^{k-1} + rK(\varphi^k) \tag{19}$$

In order to get the optimal solution of (18), we can construct an artificial time variable and solve the following equation to reach a steady state

$$\frac{\partial \varphi}{\partial t} + \frac{\partial L}{\partial \varphi} = 0 \tag{20}$$

It is easy to see that

$$\frac{\partial L}{\partial \varphi} = (u - u_0)\frac{\partial u}{\partial \varphi} - \beta \sum_{i=1}^{n} \nabla \cdot \left(\frac{\omega'(\nabla \psi_i)}{|\nabla \psi_i|} \nabla \psi_i\right) \frac{\partial \psi_i}{\partial \varphi} + \lambda \frac{\partial K}{\partial \varphi} + rK \frac{\partial K}{\partial \varphi} \tag{21}$$

We choose a fixed step size Δt and do a fixed number of the following iterations to solve (18) approximately

$$\varphi^{new} = \varphi^{old} - \Delta t \frac{\partial L}{\partial \varphi}(c^k, \varphi^{old}, \lambda^{k-1}) \tag{22}$$

The update of the variance c and the Lagrangian-multiplier λ are the same as in [5], and the algorithm process in detail can be found in [5].

5 Numerical examples

In this section, we will demonstrate the efficiency of the IMS model and compare it with the MS model. We will concentrate on two-phase ($n = 2$) and four-phase segmentation ($n = 4$).

When we choose $\omega(s) = s$, model (8) is the same as model (7). Then, clearly, the function ω does not satisfy the conditions of (13) and (15), therefore making the images smooth in all directions and leading to the disappearance of the objects.

In this paper, we adopt the function

$$\omega(s) = \sqrt{\alpha + s^2} \tag{23}$$

where $\alpha > 0$ is a constant. The function $\omega(s)$ can satisfy the conditions of (13) and (15), so we use the new energy function

$$F(c, \varphi) = \frac{1}{2}\int_{\Omega} |u - u_0|^2 \mathrm{d}x + \beta \sum_{i=1}^{n} \int_{\Omega_i} \sqrt{\alpha + |\nabla \psi_i|^2}\mathrm{d}x \tag{24}$$

As in [10], we can use the following scaling procedure to get the initial values for φ. First, we need to fix the phase number n. Then, we scale u_0 to a function between 1 and n, and take it as the initial value for φ, *i.e.*,

$$\varphi^0(x) = 1 + \frac{u_0(x) - \min\limits_{x\in\Omega} u_0}{\max\limits_{x\in\Omega} u_0 - \min\limits_{x\in\Omega} u_0} \times (n - 1) \tag{25}$$

We consider only two-dimensional gray-scale images. To complicate the segmentation process, we typically expose the original image with Gaussian distributed noise and use the polluted image as an observation data u_0. In the following section, we will use noised images of an airplane and a brain to prove the efficiency of the new model.

The first example is an airplane image. We challenge the segmentation by adding a large amount of Gaussian distributed noise to real image and take the polluted image in Fig. 2(a) (see next page) as the observation data and compare IMS model with the MS model[5]. The results are displayed in Figs. 1∼3. The convergences of $\lg\|K(\varphi^k)\|_{L^2}$ with gradient descent method for the IMS model and the MS model are plotted in Fig.1. We substitute $\beta = 0.6$ into the IMS model and $\beta = 0.1$ into the MS model. The plot shows that the IMS model converges much faster and performs better (Figs 2 and 3) than the MS model. In Fig.2, we gradually increase the regularization parameter β, to obviously reduce the boundary length of the airplane. If we continue to increase β, when $\beta = 0.6$, the airplane will disappear by the use of the MS model, but in Fig. 3, we can clearly see that the IMS model prevents the airplane from disappearing, and we can attain good segmentation and denoising. This shows that when we enlarge the penalization term parameter β, the speed of convergence also increases (Fig. 1). The MS model makes images gradually disappear (Fig. 2), but the IMS model has no such shortcoming (Fig. 3). This not only increases the speed but also preserves the shape of objects.

The next example is a numerical test on magnetic resonance imaging (MRI) by the use of the IMS model. We will illustrate 4-phase segmentation (*i.e.*, exactly four objects based on gray-scale from the original image) on the real brain image by the PCLSM with the IMS model. This image is difficult to segment due to the fact that the curves are complicated and the intensity values are not nearly constant inside each phase. The exacted four phases are depicted in Figs 4 (b), (c), (e), and (f), and Fig. 4(d) is the image after segmentation and denoising. We adopt $\beta = 0.5, r = 1 \times 10^6, \Delta t = 1 \times 10^{-8}$, and $\alpha = 10$ for the algorithm. It is not difficult to segment this image by the IMS model and algorithm, and the result is also perfect.

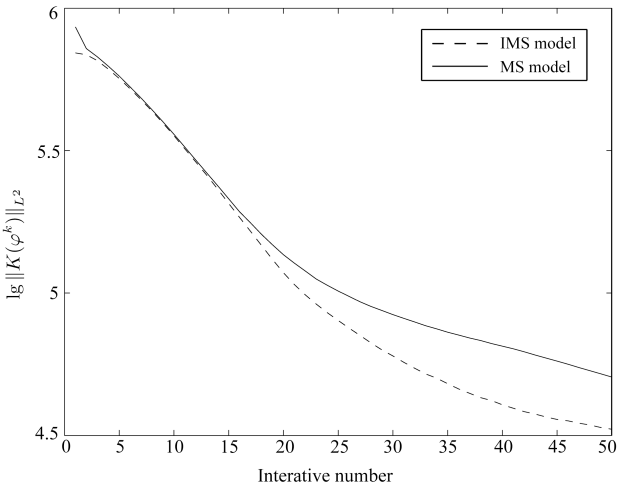

Fig. 1 A comparison of the convergence of $\lg\|K(\varphi^k)\|_{L^2}$ between the IMS model ($\beta = 0.6$) with the MS model ($\beta = 0.1$)

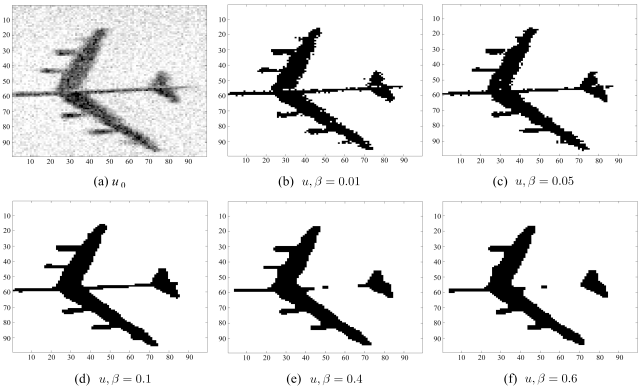

Fig. 2 Results obtained from different values of the penalization parameter β by MS model (With increasing β, the length boundary of the airplane clearly decrease. With continuously increasing β, the airplane gradually disappears.)

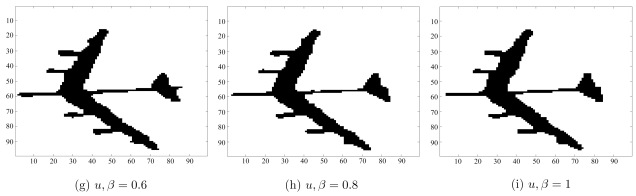

Fig. 3 Results obtained from larger values of the regularization parameter β by IMS model, $\alpha = 10$ (Though β is very large, the object shape is preserved, and the equation is also very stable.)

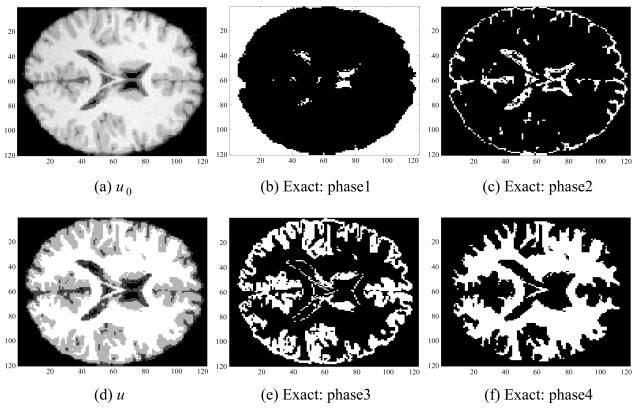

Fig. 4 The 4-phase segmentation of brain image by IMS model

6 Concluding remarks

In this paper, an IMS model is proposed and used for image segmentation and denoising. Detailed analysis and experimentation show that the IMS model can effectively prevent images from disappearing and can stabilize the equation when we increase the penalty parameter β in order to accelerate segmentation and smooth images. The IMS model is more common and reasonable than the MS model. In the future, we will try to find more proper function ω to make the IMS model more reasonable, and to improve segmentation and denoising.

References

1 Osher S, Sethian J A. Fronts propagating with curvature dependent speed: algorithms based on Hamilton-Jacobi formulations. *Journal of Computational Physics*, 1988, **79**: 12∼49

2 Tai X C, Chan T F. A survey on multiple level set methods with applications for identifying piecewise constant functions. *International Journal of Numerical Analysis and Modeling*, 2004, **1**(1): 25∼47

3 Burger M, Osher S J. A Survey on Level Set Methods for Inverse Problems and Optimal Design. CAM Report 04-02, Department of Mathematica, University of California, Los Angeles, USA, 2004

4 Osher S, Fedkiw R P. Level set methods: an overview and some recent results. *Journal of Computational Physics*, 2001, **169**(2): 463∼502

5 Lie J, Lysaker M, Tai X C. A variant of the level set method and applications to image segmentation. *Mathematics for Computation*, 2006, **75**(255): 1155∼1174

6 Lie J, Lysaker M, Tai X C. A binary level set model and some applications for Mumford-Shah image segmentation. *IEEE Transactions on Image Processing*, 2006, **15**(5): 1171∼1181

7 Lie J, Lysaker M, Tai X C. Piecewise constant level set methods and image segmentation. *Lecture Notes in Computer Science*, 2005, **3459**: 573∼584

8 Nielsen L K, Tai X C, Aannosen S I, Espedal M. A binary level set model for elliptic inverse problems with discontinuous coefficients. *International Journal of Numerical Analysis and Modeling*, 2005, **4**(1): 74∼99

9 Tai X C, Li H W. A piecewise constant level set methods for elliptic inverse problems. *Applied Numerical Mathematics*, 2007, **57**(5-7): 686∼696

10 Tai X C, Yao C H. Fast Piecewise Constant Level Set Methods (PCLSM) with Newton Updating. CAM-Report-05-52, Applied Mathematics, University of California, Los Angeles, USA, 2005

11 Mumford D, Shah J. Optimal approximation by piecewise smooth functions and associated variational problems. *Communications on Pure and Applied Mathematics*, 1989, **42**(5): 577∼685

12 Aubert G, Vese L. A variational method in image recovery. *SIAM Journal of Numerical Analysis*, 1997, **34**(5): 1948∼1979

13 Kornprobst P, Deriche R, Aubert G. Nonlinear operators in image restoration. In: Proceedings of Computer Society Conference on Computer Vision and Pattern Recognition. San Juan, Puerto Rico: IEEE, 1997. 325∼331

SONG Jin-Ping Received her master degree at College of Mathematics in University of Science and Technology of China in 1990. Now she is an associate professor at College of Mathematics and Information Science in Henan University. Her research interest covers differential equation, wavelet transform, and image processing. Corresponding author of this paper.
E-mail: songjp@henu.edu.cn

LI Shuai-Jie Master student at College of Mathematics and Information Science, Henan University. His main research interest is image processing based on PDE.
E-mail: ls-jie@163.com